A Computational Model of Grid Cells Based on Dendritic Self-Organized Learning

Conference Paper · January 2013

2 authors:

Jochen Kerdels
FernUniversität in Hagen

Gabriele Peters
FernUniversität in Hagen

A Computational Model of Grid Cells Based on Dendritic Self-Organized Learning

Jochen Kerdels, Gabriele Peters
Chair of Human-Computer Interaction, University of Hagen, Universitätsstrasse 1 , D-58097 Hagen, Germany
{Jochen.Kerdels, Gabriele.Peters}@FernUni-Hagen.de

Keywords: grid cells, model of grid formation, self organization, population coding

Abstract: In this paper we present a new computational model for *grid cells*. These cells are neurons in the entorhinal cortex of the hippocampal region that encode allocentric spatial information. They possess a peculiar, triangular firing pattern that spans the entire environment with a virtual lattice. We show that such a firing pattern can emerge from a dendritic, self-organized learning process. A key aspect of the proposed model is the hypothesis that the dendritic tree of a grid cell can behave like a sparse self organizing map that tries to cover its input space as best as possible. We argue, that the encoding scheme used by grid cells is possibly not limited to the description of spatial information and may represent a general principle on how complex information is encoded in higher level brain areas like the hippocampal region.

1 INTRODUCTION

In recent years several types of neurons were discovered in the hippocampal region, notably in the entorhinal cortex, that encode allocentric spatial information. Among those newly discovered types of neurons are so-called *grid cells*. These neurons exhibit a peculiar kind of firing pattern. Every grid cell covers the entire environment of the animal with a virtual, triangular lattice and whenever the animal passes through a vertex of this lattice, the grid cell fires. A common hypothesis suggests that groups of grid cells with lattices of different scale and orientation collectively encode a single, absolute position of the animal (McNaughton et al., 2006; Fiete et al., 2008; Moser et al., 2008).

In this paper we present a new computational model for grid cells that illustrates how the triangular firing pattern of these cells can emerge from a dendritic, self-organized learning process. A key aspect of this model is the hypothesis that the dendritic tree of a grid cell behaves like a sparse self organizing map that tries to cover its input space as best as possible. This conceptual shift from common self-organized maps on a neuronal network level to individual self-organized maps per neuron holds some interesting new perspectives on how complex, high level information may be represented within populations of neurons. We argue, that the encoding scheme used by grid cells is possibly not limited to the description of spatial information and may represent a general principle on how complex information is encoded in higher level brain areas like the hippocampal region.

The paper is organized as follows: Sections 2 and 3 will briefly summarize key elements and properties of the spatial representation in the hippocampal region in general and of grid cells in particular. In section 4 an overview of existing computational models for grid cells is given. Subsequently we introduce our own computational model in section 5 and provide experimental results in section 6 that further illustrate the properties of the proposed model. The paper ends with a more general discussion and an outlook on further research directions in sections 7 and 8.

2 SPATIAL REPRESENTATION IN THE HIPPOCAMPAL REGION

The hippocampal region[1] of the mammalian brain contains several types of neurons that encode allocentric spatial information. In 1971 O'Keefe and Dostrovsky made the discovery of *place cells* in rats (O'Keefe and Dostrovsky, 1971; O'Keefe, 1976). These cells, located in the CA1 and CA3 regions of the hippocampus, fire when the animal passes through

[1] A good overview of the hippocampal region is given in (Witter et al., 2000; van Strien et al., 2009).

specific locations in its environment. The location where a particular place cell fires is called the cell's *place field*.

In 1990 Taube et al. presented their finding of *head-direction cells* in rats (Taube et al., 1990). As their name suggests head-direction cells fire when the animal is looking in a certain, absolute direction. Head-direction cells were found in several brain regions including the postsubiculum, anterodorsal thalamus, lateral mammillary nuclei, retrosplenial cortex, lateral dorsal thalamus, striatum, and entorhinal cortex (Taube, 2009). The absolute firing direction of these cells is controlled by different, external cues such as visual landmarks. Additionally, internal self-motion information like angular head velocity is integrated to maintain head direction information when external cues are less available, e.g., when the animal moves in the dark.

Another cell type similar to place cells are *grid cells* (Fyhn et al., 2004; Hafting et al., 2005). They are located in the medial entorhinal cortex. In contrast to place cells grid cells have not one but several firing fields which are arranged in a periodic triangular grid that spans the entire environment of the animal (Fig. 1). It is commonly assumed that grid cells participate in a path integration computation that determines the absolute position of the animal in its environment using speed and direction signals as input. A more detailed description of grid cell properties and a summary of current theoretical models of grid cell formation are given in section 3 and section 4, respectively.

In addition to grid cells further investigation of the entorhinal cortex revealed the existence of grid cells colocalized with head-direction cells and *conjunctive grid × head-direction cells* (Sargolini et al., 2006) as well as *border cells* (Solstad et al., 2008). The latter being a cell type that fires whenever the animal is close to a physical border in its environment, e.g., a wall. Conjunctive grid × head-direction cells are cells with grid-cell-like firing fields that only fire at those field locations when the animal is facing in a certain direction.

3 GRID CELLS

The first detailed account of grid cells in the medial entorhinal cortex (MEC) of rats was given by Hafting et al. in (Hafting et al., 2005). Grid cells encode allocentric spatial information as they exhibit multiple discrete firing fields, i.e., they only fire when the animal moves through certain positions of its environment. The firing fields of a single grid cell are arranged in a very peculiar, triangular grid that spans the entire environment. Figure 1 depicts the firing pattern of such a grid cell while a rat is moving in a square enclosure. The trajectory of the rat is represented by the black lines, firing of the place cell at a given location is indicated by a red dot. The right side of the figure shows the spatial autocorrelation of the grid cell's firing rate map (not shown) with blue colors representing low values and red colors representing high values.

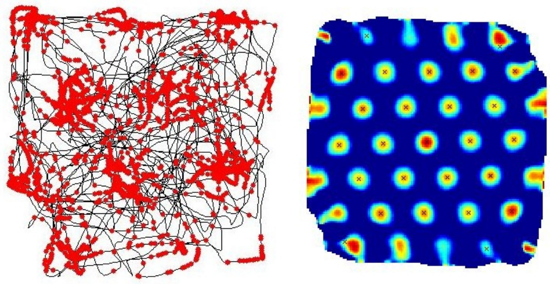

Figure 1: **Left:** the black line represents the running path of a rat. Spikes fired by a single grid cell at a certain position are marked with a red dot. **Right:** color coded spatial autocorrelation (blue: low values, red: high values) of the grid cell's rate map (not shown) verifying the periodic triangular firing pattern of the grid cell. Images by Torkel Hafting under CC BY-SA 3.0 licence.

Hafting et al. define four measures to describe the spatial properties of grid cells: *spacing*, *orientation*, *field size*, and *phase*. The spacing of a grid cell is given by the median of the distances between the central peak of the autocorrelogram and its surrounding six peaks. The orientation of a grid cell is defined as the angle between a given reference line (0 degrees) going through the central peak of the autocorrelogram and a vector from the central peak to the surrounding vertex which is nearest to the reference line in counterclockwise direction. The field size, i.e., the size of the individual fields of a grid cell, is estimated by the area covered by the central peak of the autocorrelogram using a fixed threshold as minimum value. The phase of a grid cell refers to the location of its grid vertices. The notion of a *phase* stems from the fact that co-localized grid cells exhibit similar spacing, orientation, and field size (see below), but have different locations for their firing fields. For two co-localized grid cells their relative phase shift is defined as the distance between the origin and the nearest peak in the cross-correlogram of the cells' rate maps. The average phase shift between neighboring grid cells is evenly distributed and appears to be not linked to the cell's relative positions.

A recent study by Stensola et al. analysed 968 grid cells in 15 rats covering up to 50% of the dorsoventral axis of the MEC (Stensola et al., 2012). Their findings show that the spacing of grid cells increases along the entorhinal dorsoventral axis in a discrete fashion. They indentified four[2] clusters of grid cells or *grid modules* with distinct grid spacings of 39.1, 47.9, 65.1, and 96.6 centimeter on average. Given the area covered by the measurements Stensola et al. estimate that the number of grid modules within MEC lies in the upper singe-digit range. Similar to the grid spacing, the identified grid modules also showed discrete grid orientations, i.e., grid cell orientations within a module were more similar than grid cell orientations across modules.

Although the orientation of grid cells is similar within a grid module, the orientation itself is not fixed. It is influenced by external cues, e.g., if a prominent visual cue in a circular environment is rotated by 90 degrees the orientation of the grid cells will rotate similarly (Hafting et al., 2005). A related phenomenon is reported by (Fyhn et al., 2007; Monaco and Abbott, 2011). If the environment of the animal changes significantly, the grid cells exhibit a realignment that is expressed by a change of phase and orientation. Experiments with rats in hairpin mazes indicate, that the realignment is not random but instead corresponds coherently to geometric properties of the environment (Derdikman et al., 2009).

In addition to a change of phase and orientation upon entering a novel environment, Barry et al. describe a temporary increase in spacing and field size as well as a reduction in grid regularity (Barry et al., 2012). Grid scale gradually returned to the values observed in familiar environments after 5 days with 60 minutes of exposure to the novel environment per day.

Wills et al. and Langston et al. investigated the development of head-direction cells, grid cells and place cells in young rats (Langston et al., 2010; Wills et al., 2010). They found that grid cells and place cells are present in a coarse and rudimentary form when young rat pups leave their nest for the first time[3] and start exploring their environment. In contrast, head direction cells are already in a mature state at this point of development. Grid cells and place cells stabilize their spatial representations during the first two weeks of exploration and exhibit adultlike properties when the rat reaches about 4 weeks of age.

[2]The grid spacing of a fith cluster was too large to confirm periodicity.

[3]typically at 15 to 16 days after birth

4 EXISTING COMPUTATIONAL MODELS OF GRID CELLS

In recent years a number of computational models were proposed that offer several different mechanisms for the formation of grid-like firing fields and other properties of grid cells. An extended overview of these models is given in (Giocomo et al., 2011). The existing models of grid cells can be divided into three groups: *oscillatory-interference models*, *attractor-network models*, and *models based on self-organization*.

In oscillatory-interference models it is assumed that each grid cell exhibits a somatic and several dendritic membrane-potential oscillations (Burgess et al., 2007; Zilli and Hasselmo, 2010). The frequency of the somatic oscillator is thought to correspond approximately to the so-called *theta rythm* which is a widespread periodic signal that can be EEG-captured throughout the hippocampal region of numerous mammal species including the rat. The frequency of the dendritic oscillators is modulated by running speed and direction whereas the influence of the latter is relative to a *preferred* direction specific to the particular dendritic oscillator. If these preferred directions are seperated by a multiple of 60 degrees a triangular, grid-like firing pattern is formed. An indication against oscillatory-interference models was given by (Yartsev et al., 2011) who report of grid cells in the entorhinal cortex of bats in the absence of theta oscillations.

In attractor-network models the formation of a grid-like firing pattern emerges from the activity of a local, two-dimensional, continuous attractor network (Fuhs and Touretzky, 2006; McNaughton et al., 2006; Navratilova et al., 2012). In such a network a stable, local "bump" of activity forms due to a two-dimensional, Mexican hat connectivity of individual neurons. This bump of activity can then be "moved" by the activity of several hidden layers of neurons which are connected in such a way, that each hidden layer moves the bump in a particular, preferred direction. The hidden layers are "selected" by head-direction cells corresponding to the preferred direction of the particular layer and the layer activity is modulated by the current running speed of the animal. In that way the two-dimensional continous attractor represents the position of the animal by integrating direction and speed signals. In order to generate a periodic, hexagonal firing pattern, the two-dimensional attractor network has to have the topology of a torus that is twisted along its major radius.

Models based on self-organization are less common than oscillatory-interference and attractor-network models. Kropff and Treves (Kropff and Treves, 2008) describe a model that utilizes a set of neurons that receives the signal of place cells as input. The dynamics of the set of neurons is controlled by two components. First, the neurons exhibit a form of *neuronal fatigue* that modulates the total synaptic activation of the neuron. Second, the transfer function of each neuron is controlled by two global, continually updated parameters that control the overall mean activity and sparseness. Learning of synaptic weights is performed via a hebbian learning rule. The resulting neurons show a grid-like firing pattern with similar spacing. However, the orientations exhibited by individual neurons are random contrary to experimental findings.

Mhatre et al. present a different approach using a form of self-organized learning (Mhatre et al., 2012). They postulate a type of cell called *stripe cell* that possesses a preferred direction and fires periodically when an animal moves a fixed distance along that direction. Coactivation of two stripe cells with different preferred directions occurs, when the periodic patterns of these cells projected onto each other coincide. Geometrically this coactivation is most frequent when the preferred directions of the two stripe cells are seperated by 60 degrees. Mhatre et al. use a self organizing map to learn this geometric relation among the set of stripe cells. As a result, the units of the self organizing map exhibit a grid-like firing pattern.

5 MODEL DESCRIPTION

Most of the existing grid cell models described in the previous section can explain the experimental findings quite well and provide testable predictions that can guide further experimental investigation. However, existing models are also characterized by relying on extensive assumptions about very specific cell and/or network properties, e.g., the existence of stripe cells in the model of Mhatre et al., the twisted, toroidal topology of the two-dimensional attractor-network models, or the preferred directions in the oscillatory-interference models.

We propose that the observed properties of grid cells can be explained with fewer and less specific assumptions about cell and network properties. In our model, the characteristic properties of grid cells are the result of three interacting processes. First, an input process integrates signals from head-direction cells and speed cells and generates two periodic, one-dimensional position signals. Second, the position signals are learned on a local level independently by each grid cell with a form of self-organized learning, and third, a second self-organized learning process on a network level influences and adjusts the individual learning processes on the local level.

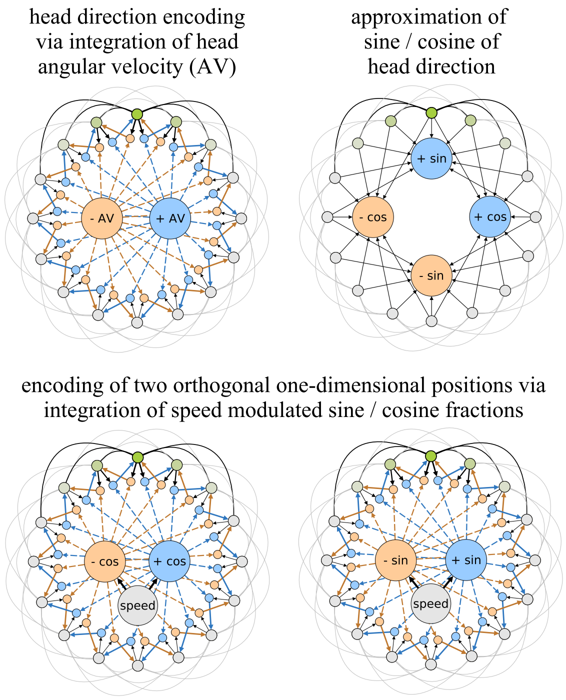

Figure 2: Model for head direction encoding and orthogonal, one-dimensional position encoding based on a one-dimensional continuous attractor network.

Input Level Like most existing grid cell models the proposed model uses the current head-direction and running speed of the animal as input signals. These signals are then integrated to generate a signal that represents the current position. We suggest, that this integration can be achieved by two one-dimensional, continuous attractor networks. One-dimensional attrator networks are commonly used to explain how the activity of head-direction cells can result from neural integration of angular velocity signals derived from the vestibular system, e.g., see (McNaughton et al., 2006). Figure 2 (top-left) depicts such a model. The outer ring of units represents head-direction cells. They have excitatory connections to neighbouring cells that decline in strength with distance (outer black and grey lines). In addition the set of head-direction cells is subject to global feedback inhibition to constrain the overall neural activity. Typically, such a network forms a single "bump" of activity at one location (green colors). This bump can be moved by a set of hidden units (blue and yellow ochre) that are asymmetrically connected to the outer units. The hidden units receive excitatory inputs from the outer units and from an input unit, e.g., an angular velocity (+/- AV) signal. The firing threshold of the hidden units is assumed to be on a level that requires inputs from both the outer units as well as the input unit in order to fire. Thus, only the hidden units "below" the current bump of activity will be active when an angular velocity signal arrives. This activity will then move the bump in the direction defined by the asymmetric connections of the particular hidden units. As a result, the network can keep track of the current head direction represented by the outer units.

In order to transform this head-direction signal into two orthogonal one-dimensional position signals the sine and cosine fractions of the particular head directions have to be approximated. This approximation can be achieved by utilizing a well-known electrotonic property of neurons. The more distant from the soma an axonal input to a dendritic tree is, the weaker is its total effect on the neuron's activity (Squire et al., 2008). Figure 2 (top-right) illustrates, how this property can be used to approximate the sine and cosine fractions of the current head direction. The head-direction cells (outer units) connect to four neurons that represent the positive and negative parts of a sine and cosine wave. The connection lengths indicate the distance to the soma and the corresponding attenuation of the input signals.

Using the sine and cosine fractions and modulating them with the current running speed of the animal, the same mechanism described for the integration of angular velocity signals can be used to generate two orthogonal, one-dimensional position signals resulting effectively in a set of periodic cartesian coordinates of the animal's position, see figure 2 (bottom). The cycle period of each coordinate is determined by the strength of the modulation through the speed signal.

Local Level The periodic position signal described in the previous section is the input to the grid cells of the proposed model. Considering the increasing evidence in recent years about the computational capabilities of dendritic trees (Sjstrm et al., 2008) we argue that a single neuron – in this case a grid cell – can learn to represent different inputs within separate sections of its dendritic tree. A possible mechanism that could facilitate such a local, dendritic representation are, e.g., dendritic spikes. As a computational model of such a dendritic learning process we adopted the *growing neural gas* (GNG) described in (Fritzke, 1995). In this context the individual units of the GNG are thought to be local sections of the dendritic tree of a grid cell. The adapted GNG approach can be summarized as follows:

The dendritic tree D of a grid cell is described as a set of dendritic subsections $d \in D$ that each have a reference vector $w_d \in \mathbb{R}^n$ and an accumulated error $e_d \in \mathbb{R}$. The reference vector has the dimension n of the grid cell's input – in this case the concatenation of the two one-dimensional position vectors. The structure of the dendritic tree is implicitly described by a set of edges $c \in C$ that describe the neighbourhood relation that develops between dendritic subsections. In addition each edge c has an age $t_c \in \mathbb{N}$ which is initialized with 0. In the beginning a grid cell has only two dendritic subsections connected by a single edge. The reference vectors of these dendritic subsections are initialized with random values. Each input x to a grid cell is then processed in the following way:

Find the two dendritic subsection s_1 and s_2 that have the smallest distance to the input x:

$$s_1 := \underset{d_i \in D}{argmin} \, \|w_{d_i} - x\|$$
$$s_2 := \underset{d_j \in D \setminus \{s_1\}}{argmin} \, \|w_{d_j} - x\|$$

If there is no edge between s_1 and s_2 add one:

$$C := C \cup \{(s_1, s_2)\}$$

Reset the age of the edge between s_1 and s_2 to 0:

$$t_{(s_1,s_2)} = 0$$

Increase the accumulated error of s_1 with the quadratic distance between the reference vector of s_1 and the input x:

$$e_{s_1} \mathrel{+}= \|w_{s_1} - x\|^2$$

Adapt the reference vectors of s_1 and all dendritic subsections that are connected via an edge with s_1:

$$\begin{aligned} w_{s_1} &\mathrel{+}= \varepsilon\,(x - w_{s_1}) \\ w_d &\mathrel{+}= \mu \cdot \varepsilon\,(x - w_d\,), \;\; d \in \{a | \, (s_1, a) \in C, a \in D\} \end{aligned}$$

Increase the age of all edges that were "used":

$$t_{(s_1,d)} \mathrel{+}= 1, \;\; d \in \{a | \, (s_1, a) \in C, a \in D\}$$

If the age of an edge if above a given threshold t_{max} the edge is deleted. If this results in a dendritic subsection that is isolated, the dendritic subsection is removed too.

Has the number of inputs reached a multiple of a given parameter λ and is the current number of dendritic subsections smaller than a desired maximum number of dendritic subsections d_{max} then a new dendritic subsection p will be added to the grid cell. For this purpose the dendritic subsection q_1 with the biggest accumulated error is selected as well as the dendritic subsection q_2 with the biggest accumulated error that is connected to q_1:

$$q_1 := \underset{d_i \in D}{argmax}\, e_{d_i}$$

$$q_2 := \underset{d_j \in \{a|(q_1,a) \in C, a \in D\}}{argmax} e_{d_j}$$

The reference vector w_p of the new dendritic subsection p is interpolated between the reference vectors of q_1 and q_2:

$$w_p := (w_{q_1} + w_{q_2})/2$$

The accumulated errors of q_1 and q_2 are reduced and the accumulated error e_p of the new dendritic subsection is interpolated between the reduced errors of q_1 and q_2:

$$\begin{aligned} e_{q_1} &-= \alpha e_{q_1} \\ e_{q_2} &-= \alpha e_{q_1} \\ e_p &:= (e_{q_1} + e_{q_2})/2 \end{aligned}$$

The edge between q_1 and q_2 is removed and new edges between q_1 and p as well as q_2 and p are inserted:

$$\begin{aligned} C &:= C \setminus \{(q_1, q_2)\} \\ C &:= C \cup \{(q_1, p), (q_2, p)\} \end{aligned}$$

Finally, all accumulated errors are reduced by a small fraction:

$$e_d -= \beta e_d, \;\; d \in D.$$

Using this procedure each grid cell will try to cover the input space with its dendritic subsections as best as it can, i.e., reducing the total error between input vectors and reference vectors. This error minimizing property of the GNG results in a characteristic triangular pattern – a Delaunay triangulation of the input space.

Network Level The process described in the previous subsection generates a grid-like firing pattern for each grid cell. The spacing of this pattern is determined by the distance covered by one period of the input signal and the number of dendritic subsections of the grid cell. The phase and orientation of the grid cells are determined by the random initialization of the initial two dendritic subsections of each grid cell. As the orientation of real grid cells is not random, we introduce a network level process that aligns the orientation of the grid cells in our model by influencing the GNG process described in the previous section.

The network level process is similar to the GNG process of the individual grid cells. We define for every grid cell $g \in G$ an activity a_g using the distances between the input vector x and the reference vectors of the two dendritic subsections g_{s_1} and g_{s_2} of g that were closest to the input:

$$a_g := 1 - \frac{\|w_{g_{s_1}} - x\|}{\|w_{g_{s_2}} - x\|}$$

In addition we define a set of edges K between grid cells that is initially empty. Each edge $k \in K$ has an age $t_k \in \mathbb{N}$ which is initialized with 0. Each input x is processed on the network level as follows:

Identify the two grid cells h_1 and h_2 that are most active:

$$h_1 := \underset{g_i \in G}{argmax}\, a_{g_i}$$

$$h_2 := \underset{g_j \in G \setminus \{h_1\}}{argmax}\, a_{g_j}$$

If there is no edge between h_1 and h_2 add one:

$$K := K \cup \{(h_1, h_2)\}$$

Reset the age of the edge between h_1 and h_2 to 0:

$$t_{(h_1,h_2)} = 0$$

Temporarily increase the adaptation rate ε of grid cell h_1 and of all grid cells connected to h_1:

$$\begin{aligned} \varepsilon_{h_1} &+= \delta \\ \varepsilon_g &+= \delta, \;\; g \in \{a|\,(h_1,a) \in K, a \in G\} \end{aligned}$$

Increase the age of all edges that link to grid cell $h1$:

$$t_{(h_1,g)} += 1, \;\; g \in \{a|\,(h_1,a) \in K, a \in G\}$$

If the age of an edge if above a given threshold t_{max} the edge is deleted.

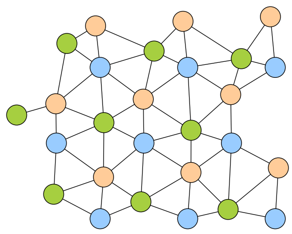

Figure 3: Illustration of the alignment process on the network level. Equally colored circles represent the firing fields of a single grid cell. Edges represent implicit connections between the firing field based on network level edges.

This adaptation of the GNG process on the network level aligns the grid cell orientations. Figure 3 illustrates how this alignment is achieved. If an edge between two grid cells is created on the network level this edge implicitly connects all neighbouring firing fields of these two grid cells. If the firing field of a grid cell is closest to an input and thus the grid cell is most active the neighboring firing fields of other grid cells are "dragged" in the direction of the active firing field as their adaptation rate is temporarily increased for the corresponding input. Thus, similar to the dendritic subsections on the local level, the grid cells on the network level also try to cover the input space as best as possible resulting in a distribution of grid cell patterns that favours an alignment of grid orientations.

6 EXPERIMENTS

In order to explore the properties of the proposed model we implemented the model and conducted a first series of experiments. In our experimental setup we varied the number of dendritic subsections per grid cell and the total number of grid cells. During the initial learning phase we generated input vectors from random positions. For each spatial dimension the input vector had 64 bins with a broad "bump" of activity across 40 bins at a random location wrapping around vector boundaries if necessary. The use of random positions as inputs to the developing grid cells can be motivated by the fact that even before rat pups start to explore their environment, cells with grid-like firing properties are already present in a coarse form (s. section 3). After the initial learning phase, we used real movement data of a rat foraging for 10 minutes in a $1\text{m} \times 1\text{m}$ box resulting in 30000 position inputs. The data was recorded and provided by Sargolini et al.[4]

To facilitate a smooth transition between a fast initial learning rate and a subsequent slower rate, the inital learning rate ε_{init} is kept constant for t_{wait} time steps and then successively reduced over a time period of t_{trans} to a value of ε_{idle}:

$$\varepsilon_t = \varepsilon_{init} \cdot \left(\frac{\varepsilon_{idle}}{\varepsilon_{init}}\right)^{\frac{t-t_{wait}}{t_{trans}}}$$

In the same way the network level adaption rate δ was slightly reduced, albeit remaining on a higher level then the adaption rate of the local level. The parameters used for the initial learning phase are equal to those used in (Fritzke, 1995). The subsequent lower learning rates were reduced by one order of magnitude.

Figures 4, 5, and 6 illustrate the activity of individual grid cells (rows) with 9 (fig. 4), 16 (fig. 5) and 25 (fig. 6) dendritic subsections in groups of 5, 40, and 100 grid cells. The left column shows the path of the rat (black lines) and simulated spikes of the particular grid cell (red dots). The spikes were simulated with a gaussian probability propotional to the grid cells activity a_g. The middle column shows the averaged rate map of the grid cell and the right column shows the autocorrelogram of the rate map (blue colors represent low values, red colors represent high values). Both maps were generated according to the methods proposed by (Sargolini et al., 2006). The figures illustrate that spacing and firing field size of the simulated grid cells is only dependent on the number

[4] data is available at http://www.ntnu.no/cbm/gridcell

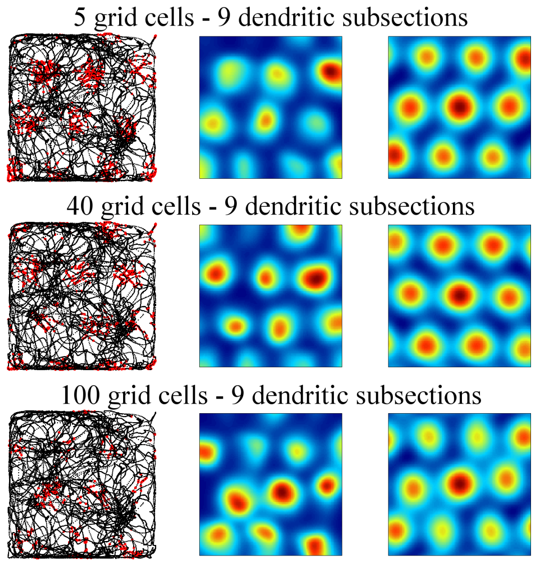

Figure 4: Each row shows the activation of a single, simulated grid cell with 9 dendritic subsections in a group of 5, 40, and 100 grid cells. The left side shows the path of the rat (black lines) and simulated spikes of the grid cell (red dots). The right side shows the autocorrelogram (central portion) of the grid cell's rate map (middle column).

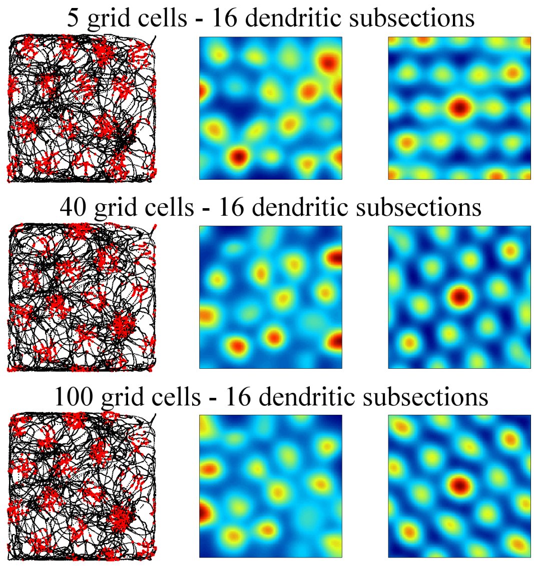

Figure 5: Activity of simulated grid cells with 16 dendritic subsections in groups of 5, 40, and 100 grid cells. Illustration corresponding to figure 4.

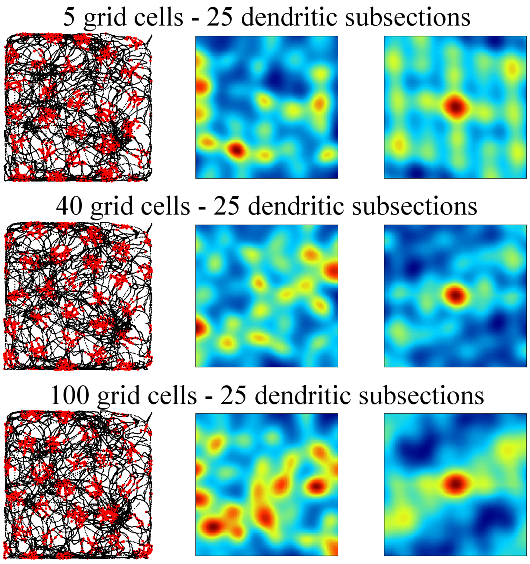

Figure 6: Activity of simulated grid cells with 25 dendritic subsections in groups of 5, 40, and 100 grid cells. Illustration corresponding to figure 4.

of dendritic subsections, whereas the number of grid cells per group has no influence. Well formed, triangular firing patterns were achieved by grid cells with 9 and 16 dendritic subsections. Grid cells with 25 or more (not shown) dendritic subsections did not yield a proper triangular pattern. However, the spike map still shows a regular, almost triangular firing pattern that could in principle still serve as a means to encode spatial information in a grid-like way.

Figure 7 illustrates the alignment process of grid cell orientations on the network level. In the beginning grid cell orientations cover the whole spectrum of orientations in a 60 degree window with a slight emphasis of the orientations around 20 and 30 degrees. Gradually over time the grid cells align their orientations to a common orientation of about 30 degrees. The orientation of the grid cells was determined as proposed by (Sargolini et al., 2006).

A second set of experiments using 170 minutes of rat movement data as input without an initial phase of random inputs yielded similar results. However, the learning rates had to be reduced by two orders of magnitude to result in a stable formation of grid patterns.

7 DISCUSSION

We presented a computational model of grid cells that is capable to generate the peculiar, triangular firing pattern observed in real grid cells and that provides an

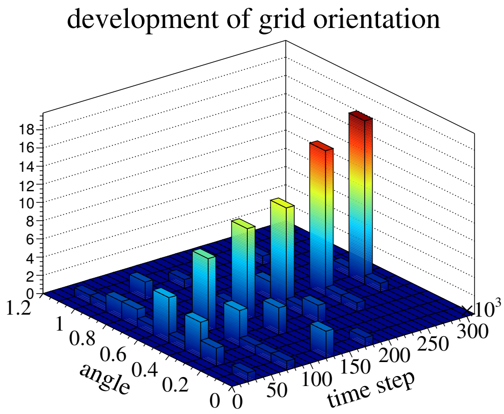

Figure 7: Development of grid cell orientation within 300.000 time steps. The group of 20 grid cells gradually aligns their orientations to a common value of about 30 degrees.

explanation how a group of grid cells can align their orientations with a self-organizing process on a network level. In addition to this, the model facilitates plausible argumentations to account for other properties of grid cells reported in section 3:

- Although spacing and orientation of co-localized grid cells are similar, they typically differ in their phase. This is also true for the presented model as the phase of a model grid cell is predominantly determined by the random, initial conditions of the first two dendritic subsections. The connections made to other grid cells on the network level are activity-based and not location-based.
- The entorhinal cortex contains discrete grid cell modules that have separate and distinct grid spacings. In the current model, the grid spacing can be influenced by the number of dendritic subsections or by the level of speed modulation of the two one-dimensional attractor-networks that generate the orthogonal, periodic input to our grid cells.
- The sudden realignment of the grid orientation and phase when an animal enters a new environment can be explained on the input level. A realignment of the head-direction cells affects immediately the four neurons that approximate the sine and cosine fractions effectively rotating the coordinate system of the model grid cells.
- The reported increase in the size of grid cells could reflect a change in the speed modulation of the two input attractor networks. If, e.g., the speed signal is in part determined by some form of optical flow and in part determined by internal, self-motion signals, a new environment may re-

quire some adjustment before optical flow and internal self-motion signals produce a coherent signal again.

- Grid cells which are already present in a coarse and rudimentary form in young rats even before they start exploring their environment can be explained by random position inputs generated during development.

Irrespective of these specific aspects regarding grid cells the idea of a dendritic self-organizing map has itself some intriguing consequences. Commonly, the units of a self-organizing map (SOM) represent single classes. In order to increase the "resolution" of a SOM more units must be added. But the more units are present in a SOM, the less inputs will be directed towards each individual unit. As fewer and fewer inputs reach individual units, learning of new inputs becomes increasingly difficult. Additionally, if the input is high-dimensional, the "curse of dimensionality" will lead to a weak discrimination between the individual units of the SOM. This contrasts the way how grid cells encode information. Instead of representing a single region of the input space they sample the whole input space at regular intervals, thus representing many regions, i.e., many classes, at once. In order to identify a specific region of the input space, grid cells of different groups with different orientation and spacing form a population code that uniquely identifies the particular region. As each cell has only a few units, i.e., dendritic subsections, in their local SOM they suffer less from the curse of dimensionality. Furthermore, a grid cell encoding of information may be metabolically more efficient than the encoding represented by a common SOM. Grid cells cover the whole input space and are to that effect more frequently active than cells of a SOM which may be only rarely used but have to be maintained anyway.

8 CONCLUSIONS AND OUTLOOK

We have presented a plausible computational model of grid cells using a dendritic self-organizing map as one of its core components. The model is not only able to generate the peculiar, triangular firing pattern of grid cells, but is also able to provide plausible arguments that can account for several other phenomena observed in the context of grid cells.

We argue that the way how grid cells encode spatial information may represent a more general concept of how high-level information is processed in the brain. It appears promising to investigate how other input modalities can be represented by a population code of dendritic SOMs. These modalities include high level feature descriptions of images, sound or more abstract signals like the posture of the body.

REFERENCES

Barry, C., Ginzberg, L. L., OKeefe, J., and Burgess, N. (2012). Grid cell firing patterns signal environmental novelty by expansion. *Proceedings of the National Academy of Sciences*, 109(43):17687–17692.

Burgess, N., Barry, C., and O'Keefe, J. (2007). An oscillatory interference model of grid cell firing. *Hippocampus*, 17(9):801–812.

Derdikman, D., Whitlock, J. R., Tsao, A., Fyhn, M., Hafting, T., Moser, M.-B., and Moser, E. I. (2009). Fragmentation of grid cell maps in a multicompartment environment. *Nat Neurosci*, 12(10):1325–1332.

Fiete, I. R., Burak, Y., and Brookings, T. (2008). What grid cells convey about rat location. *The Journal of Neuroscience*, 28(27):6858–6871.

Fritzke, B. (1995). A growing neural gas network learns topologies. In *Advances in Neural Information Processing Systems 7*, pages 625–632. MIT Press.

Fuhs, M. C. and Touretzky, D. S. (2006). A spin glass model of path integration in rat medial entorhinal cortex. *The Journal of Neuroscience*, 26(16):4266–4276.

Fyhn, M., Hafting, T., Treves, A., Moser, M.-B., and Moser, E. I. (2007). Hippocampal remapping and grid realignment in entorhinal cortex. *Nature*, 446(7132):190–194.

Fyhn, M., Molden, S., Witter, M. P., Moser, E. I., and Moser, M.-B. (2004). Spatial representation in the entorhinal cortex. *Science*, 305(5688):1258–1264.

Giocomo, L., Moser, M.-B., and Moser, E. (2011). Computational models of grid cells. *Neuron*, 71(4):589 – 603.

Hafting, T., Fyhn, M., Molden, S., Moser, M.-B., and Moser, E. I. (2005). Microstructure of a spatial map in the entorhinal cortex. *Nature*, 436(7052):801–806.

Kropff, E. and Treves, A. (2008). The emergence of grid cells: Intelligent design or just adaptation? *Hippocampus*, 18(12):1256–1269.

Langston, R. F., Ainge, J. A., Couey, J. J., Canto, C. B., Bjerknes, T. L., Witter, M. P., Moser, E. I., and Moser, M.-B. (2010). Development of the spatial representation system in the rat. *Science*, 328(5985):1576–1580.

McNaughton, B. L., Battaglia, F. P., Jensen, O., Moser, E. I., and Moser, M.-B. (2006). Path integration and the neural basis of the 'cognitive map'. *Nat Rev Neurosci*, 7(8):663–678.

Mhatre, H., Gorchetchnikov, A., and Grossberg, S. (2012). Grid cell hexagonal patterns formed by fast self-organized learning within entorhinal cortex. *Hippocampus*, 22(2):320–334.

Monaco, J. D. and Abbott, L. F. (2011). Modular realignment of entorhinal grid cell activity as a basis for hippocampal remapping. *The Journal of Neuroscience*, 31(25):9414–9425.

Moser, E. I., Kropff, E., and Moser, M.-B. (2008). Place cells, grid cells, and the brain's spatial representation system. *ANNUAL REVIEW OF NEUROSCIENCE*, 31:69–89.

Navratilova, Z., Giocomo, L. M., Fellous, J.-M., Hasselmo, M. E., and McNaughton, B. L. (2012). Phase precession and variable spatial scaling in a periodic attractor map model of medial entorhinal grid cells with realistic after-spike dynamics. *Hippocampus*, 22(4):772–789.

O'Keefe, J. (1976). Place units in the hippocampus of the freely moving rat. *Experimental Neurology*, 51(1):78 – 109.

O'Keefe, J. and Dostrovsky, J. (1971). The hippocampus as a spatial map. preliminary evidence from unit activity in the freely-moving rat. *Brain Research*, 34(1):171 – 175.

Sargolini, F., Fyhn, M., Hafting, T., McNaughton, B. L., Witter, M. P., Moser, M.-B., and Moser, E. I. (2006). Conjunctive representation of position, direction, and velocity in entorhinal cortex. *Science*, 312(5774):758–762.

Sjstrm, P. J., Rancz, E. A., Roth, A., and Husser, M. (2008). Dendritic excitability and synaptic plasticity. *Physiological Reviews*, 88(2):769–840.

Solstad, T., Boccara, C. N., Kropff, E., Moser, M.-B., and Moser, E. I. (2008). Representation of geometric borders in the entorhinal cortex. *Science*, 322(5909):1865–1868.

Squire, L., Bloom, F., Spitzer, N., Squire, L., Berg, D., du Lac, S., and Ghosh, A. (2008). *Fundamental Neuroscience*. Fundamental Neuroscience Series. Elsevier Science.

Stensola, H., Stensola, T., Solstad, T., Froland, K., Moser, M.-B., and Moser, E. I. (2012). The entorhinal grid map is discretized. *Nature*, 492(7427):72–78.

Taube, J. (2009). Head direction cells. *Scholarpedia*, 4(12):1787.

Taube, J., Muller, R., and Ranck, J. (1990). Head-direction cells recorded from the postsubiculum in freely moving rats. i. description and quantitative analysis. *The Journal of Neuroscience*, 10(2):420–435.

van Strien, N. M., Cappaert, N. L. M., and Witter, M. P. (2009). The anatomy of memory: an interactive overview of the parahippocampal-hippocampal network. *Nat Rev Neurosci*, 10(4):272–282.

Wills, T. J., Cacucci, F., Burgess, N., and O'Keefe, J. (2010). Development of the hippocampal cognitive map in preweanling rats. *Science*, 328(5985):1573–1576.

Witter, M. P., Wouterlood, F. G., Naber, P. A., and van Haeften, T. (2000). Anatomical organization of the parahippocampal-hippocampal network. *Annals of the New York Academy of Sciences*, 911(1):1–24.

Yartsev, M. M., Witter, M. P., and Ulanovsky, N. (2011). Grid cells without theta oscillations in the entorhinal cortex of bats. *Nature*, 479(7371):103–107.

Zilli, E. A. and Hasselmo, M. E. (2010). Coupled noisy spiking neurons as velocity-controlled oscillators in a model of grid cell spatial firing. *The Journal of Neuroscience*, 30(41):13850–13860.